J Med Syst (2017) 41: 157
DOI 10.1007/s10916-017-0799-z

IMAGE & SIGNAL PROCESSING

Image Retrieval Based on Local Mesh Vector Co-occurrence Pattern for Medical Diagnosis from MRI Brain Images

A. Jenitta[1] · **R. Samson Ravindran**[2]

Received: 31 March 2017 / Accepted: 14 August 2017 / Published online: 31 August 2017

Abstract In modern health-care, for evidence-based diagnosis, there is a requirement for an efficient image retrieval approach to retrieve the cases of interest that have similar characteristics from the large image databases. This paper presents a feature extraction approach that aims at extracting texture features present in the medical images using Local Pattern Descriptor (LPD) and Gray-level Co-occurrence Matrix (GLCM). As a main contribution, a novel local pattern named Local Mesh Vector Co-occurrence Pattern (LMVCoP) has been proposed by concatenating the Local Mesh Co-occurrence Pattern (LMCoP) and the Local Vector Co-occurrence Pattern (LVCoP). The fusion of GLCM with the Local Mesh Pattern (LMeP) and the Local Vector Pattern (LVP) produces LMCoP and LVCoP respectively. The LMVCoP method has been investigated on the Open Access Series of Imaging Studies (OASIS): a Magnetic Resonance Imaging (MRI) brain image database. LMVCoP descriptor achieves 87.57% of ARP and 53.21% of ARR which are higher than the existing methods of LTCoP, PVEP, LBDP, LMeP and LVP. The LMVCoP method enhances the retrieval results of LMeP/LVP from 81.36%/83.52% to 87.57% in terms of ARP on OASIS MRI brain database.

This article is part of the Topical Collection on *Image & Signal Processing*

✉ A. Jenitta
jenittaiecw@gmail.com

[1] Department of Electronics and Communication Engineering, Idhaya Engineering College For Women, Villupuram (Dt), Chinnasalem, Tamilnadu 606 201, India

[2] Department of Electronics and Communication Engineering, Mahendra Engineering College, Namakkal(Dt), Mallasamuthram, Tamilnadu, India

Keywords Image processing · MRI brain images · Medical diagnosis · Texture based image retrieval · Local mesh vector co-occurrence pattern

Introduction

Every day massive amount of medical images is acquired and preserved as databases in health care centers for future references, disease diagnostics and for proper treatment. Physician uses these large medical image data as the modern frontier of the medical field and improves the quality of medical treatment. Many referring physicians also show a great interest for direct access to medical image data and to discuss with their hospital colleagues by retrieving the required image immediately and have the chance to confer the case collaboratively with other specialists for successful decision making. Healthy people also show interest to have a master medical check up periodically which increases the accumulation of medical images in the hospitals. Hence, there is a need to find the most clinically relevant images in response to specific information required. Content-Based Image Retrieval (CBIR) focused to follow a line of investigation to fulfill this requirement. Where CBIR is a well-known technology used to organize an image database by their features (contents) and to search it according to the requirement. Ultimately, the Content-Based Medical Image Retrieval (CBMIR) attracts extensive attention in the research community by its significant clinical benefits and the pace of its research is still rising.

Duncan and Ayache listed out four important challenges should be faced while analysing medical images [1]. They are: (1) addressing the biological problems, (2) Characterizing different imaging modalities, (3) identifying proper techniques

for geometrical analysis of both normal and abnormal information, and (4) integrating with other communities' research activities to provide new opportunities. Lakovidis et al. [2] extracted multi-scale statistical features using a 2D discrete wavelet transform and by clustering those features into small patterns, by comprising the sets of these smaller patterns and representing as complex patterns. Rahman et al. [3] proposed a multimodal query expansion method by integrating textual keywords and visual data. Bag-of-features [4] such as Scale Invariant Feature Transform (SIFT) and image patches have been modelled using the quadratic programming assignment and analyzed by both the strong and weak classifiers on the ImageCLEF, CT and the basal-cell carcinoma datasets by Wang et al. in 2011. Followed by, Quellec et al. [5] introduced a content-based heterogeneous information retrieval framework using a Bayesian network. Then Cao et al. [6] proposed a multimodal medical image retrieval approach using the statistical graphic model and deep learning. To overcome the limitation of semantic gap, the authors introduced an extended probabilistic latent semantic analysis model by combining both the visual and textual information from medical images for cancer care. And to derive the missing modality, they developed a Boltzmann machine-based multimodal learning model. Next, saliency based folding method has been developed by employing Local Binary Patterns (LBP) and Support Vector Machines (SVM) in 2015 [7]. Albarqouni et al. [8] used Convolutional Neural Networks (CNN) through additional crowd sourcing layer (AggNet) for deep learning for Mitosis detection from the breast cancer histology images. Later, fuzzy aggregation operators based dental diagnosis has been performed dental X-ray images [9]. Shortly, Speeded Up Robust Feature (SURF) descriptor has been developed on the lung images for implementing an efficient CBMIR [10]. On the Image Retrieval in Medical Applications (IRMA) dataset, Radon Bar-Code (RBC), Convolutional Neural Network Code (CNNC) and Regions of Interest (ROI) based matching has been investigated along with the cross-correlation method [11]. Recently, Expectation Maximization (EM) and Fuzzy C-Means (FCM) were implemented on MRI brain images [12].

Feature extraction takes a vital role of extracting the fine features of images for better image retrieval. The efficiency of the retrieval can be augmented by choosing the perfect feature extraction technique. Furthermore, the features present in the medical images are complex; anatomical structures are highly irregular and multimodality image' structures are misaligned. To face this challenge, a novel texture based local pattern descriptor has been proposed in this paper to extract features from MRI brain images and to retrieve them automatically whenever needed.

The evolution of local patterns is as follows: the Local Binary Pattern (LBP) [13] has been initially intended for texture description. Subsequently, Tan and Triggs [14] provided the Local Ternary Pattern (LTP) as an expansion of the LBP. Later, Murala et al. proposed the Local Tetra Pattern (LTrP) [15] for facial image recognition and the Directional Binary Wavelet Pattern (DBWP) [16] for MRI, CT and facial image retrieval. After that, Murala and Wu proposed the Peak Valley Edge Patterns [17] and the Local Mesh Pattern (LMeP) [18] on biomedical images. Later, the Local Vector Pattern (LVP) [19] has been developed for facial feature extraction. Then Yesubai and Ravi proposed the Local Mesh Co-occurrence Pattern (LMCoP) on natural scenery images [20]. Thus, the local patterns have gained much attention in the facial recognition area than the medical field. It stimulates the idea of introducing a new hybrid local pattern LMVCoP for medical image retrieval application.

The proposed method

This section describes the proposed CBMIR based on LMVCoP technique in more detail. Figure 1 depicts the flow of the proposed system. The steps followed in this work are listed below:

Step 1: Pre-processing Given image is first pre-processed to synchronize the content in a database and thus create effective feature extraction from the images based on the same basis. The image is initially converted into a gray-scale image and resized into 256 × 256 pixels. The image is then normalized using contrast enhancement of adaptive histogram equalization. Since adaptive histogram equalization distributes the most repeated intensity values and transforms the lower local contrast into higher contrast effectively, this method is used here. Followed by, the process of smoothing that reduces the noise was performed to produce a more accurate intensity surface. Since Gaussian filter is very effective for removing Gaussian noise, reducing edge blurring, rotationally symmetric and computationally efficient for MRI brain images, Gaussian smoothing is used in this work for a removal of small unconnected objects and to adjust for residual between-subject neuro-anatomic differences.

Step 2: Extracting features using local vector co-occurrence pattern Given a pre-processed local sub-region I, α is the index angle, g_c is the center pixel in I, D is the distance between the centre pixel and its neighboring pixels in the

α direction. First, a vector that denoted as $\boldsymbol{V_{\alpha,D}(g_c)}$ is calculated by

$$V_{\alpha,D}(g_c) = \left(I(g_{\alpha,D}) - I(g_C)\right) \quad (1)$$

Then, the $\boldsymbol{LVP_{N,R,\alpha}(g_c)}$, in the α direction is encoded as

$$LVP_{N,R,\alpha}(g_c) = T\left(V_{\alpha,D}(g_{1,R}), V_{\alpha+45^\circ,D}(g_{1,R}), V_{\alpha,D}(g_c), V_{\alpha+45^\circ,D}(g_c)\right), \ldots, T\left(V_{\alpha,D}(g_{N,R}), V_{\alpha+45^\circ,D}(g_{N,R}), V_{\alpha,D}(g_c), V_{\alpha+45^\circ,D}(g_c)\right) \quad (2)$$

Where $N = 1, 2, \ldots, M; R = 1,$

$T(\cdot, \cdot)$ is defined as

$$T\left(V_{\alpha,D}(g_{N,R}), V_{\alpha+45^\circ,D}(g_{N,R}), V_{\alpha,D}(g_c), V_{\alpha+45^\circ,D}(g_c)\right) = \begin{cases} 1, & if\ V_{\alpha+45^\circ,D}(g_{N,R}) - \left(\frac{V_{\alpha+45^\circ,D}(g_c)}{V_{\alpha,D}(g_c)} \times V_{\alpha,D}(g_{N,R})\right) \geq 0 \\ 0, & else \end{cases} \quad (3)$$

Next, the $\boldsymbol{LVP_{N,R}(g_c)}$, is computed by combining four 8-bit binary patterns. For every center pixel of I, a 32-bit binary pattern is generated.

$$LVP_{N,R}(g_c) = LVP_{N,R,\alpha}(g_c), |\alpha = 0^\circ, 45^\circ, 90^\circ, 135^\circ \quad (4)$$

Finally, the resultant LVP map is computed using GLCM, where, $\boldsymbol{M}$ is a matrix whose size $M_x \times M_y$ is equal to the number of gray-levels *0 to M-1*. At an angle θ and d distance, the variation between gray level i and j, has been calculated and represented as the matrix element $\boldsymbol{C(i,j|d,\theta)}$. $C_x(i)$ and $C_y(j)$ are computed by

$$C_x(i) = \sum_{i=0}^{M_x-1} C(i,j) \quad (5)$$

$$C_y(j) = \sum_{j=0}^{M_y-1} C(i,j) \quad (6)$$

Once the Co-occurrence matrix has been formed, the following Haralick texture features can be computed by

$$CONTRAST = \sum_{I=0}^{m-1} n^2 \left\{ \sum_{j=0}^{M_x-1} \sum_{j=0}^{M_y-1} C(i,j) \right\} \quad (7)$$

where $n = |i-j|, i \neq j$

$$CORRELATION = \sum_{i=0}^{M_x-1} \sum_{j=0}^{M_y-1} \frac{\{i \times j\} \times C(i,j) - \left\{\mu_x \times \mu_y\right\}}{\sigma_x \times \sigma_y} \quad (8)$$

where mean μ_x and μ_y take the average level of intensity of given input such as

$$\mu_x = \sum_{i=0}^{M_x-1} i C_x(i) \quad (9)$$

$$\mu_y = \sum_{j=0}^{M_y-1} j C_y(j) \quad (10)$$

whereas the variance σ_x and σ_y describe the variation of intensity around the mean.

$$Energy = \sum_{i=0}^{M_x-1} \sum_{j=0}^{M_y-1} C^2(i,j) \quad (11)$$

$$Homogeneity = \sum_{i=0}^{M_x-1} \sum_{j=0}^{M_y-1} \frac{C(i,j)}{1 + |i-j|} \quad (12)$$

Step 3: Extracting features using local mesh co-occurrence pattern Given a pre-processed local sub-region I, the relationship among the surrounding neighbours of the centre pixel $I^1(g_n)$ is computed by

$$I^1(g_n) = I(g_m) - I(g_n) \quad (13)$$

where $n = 1, 2, \ldots, 8$. Then the LMeP can be calculated by

$$LMeP^M_{N,R} = \sum_{n=1}^{N} 2^{(n-1)} \times f_1(g_m - g_n) \quad (14)$$

$$m = 1 + mod((n + N + M - 1), N) \quad \forall M = 1, 2, \ldots, \left({}^{N}/_{2}\right) \quad (15)$$

After computing the LMeP, apply GLCM on the resultant LMeP map using Eqs. (5–12).

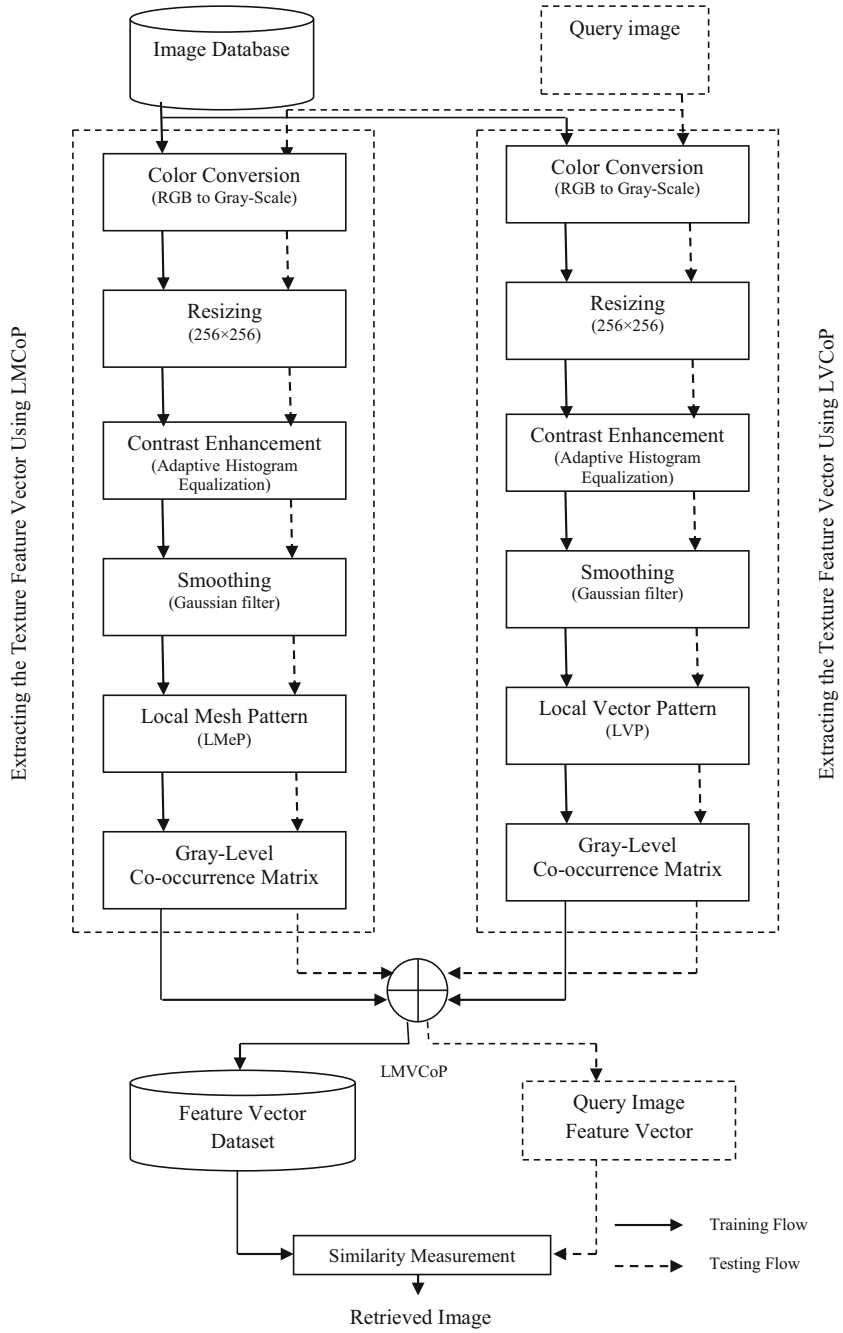

Fig. 1 Flowchart of the proposed system

Step 4: Computing local mesh vector co-occurrence pattern The local pattern results are combined using the sum rule. For Example, LMCoP denotes GLCM of LMeP, similarly LVCoP denotes GLCM of LVP, and then the combined approach of these two patterns is abbreviated as LMVCoP, which can be written as:

$$LMVCoP = wLMCoP + (1-w)LVCoP \tag{16}$$

where, w is a weighted parameter that ranges from 0.1 to 0.9. The relationship between LMCoP and LVCoP can be investigated by changing w, and the performance of LMVCoP can also be evaluated. In this work, initially, all the tests were performed for $w = 0.2$

Step 5: Retrieval Once the proposed model LMVCoP is trained for all the medical images of the given dataset, the feature vectors are stored as a feature dataset with reduced dimension. Then, the step, retrieval is performed. The similarity measurement is computed between the feature vectors of feature dataset and the feature vector of query image based on Squared Euclidean

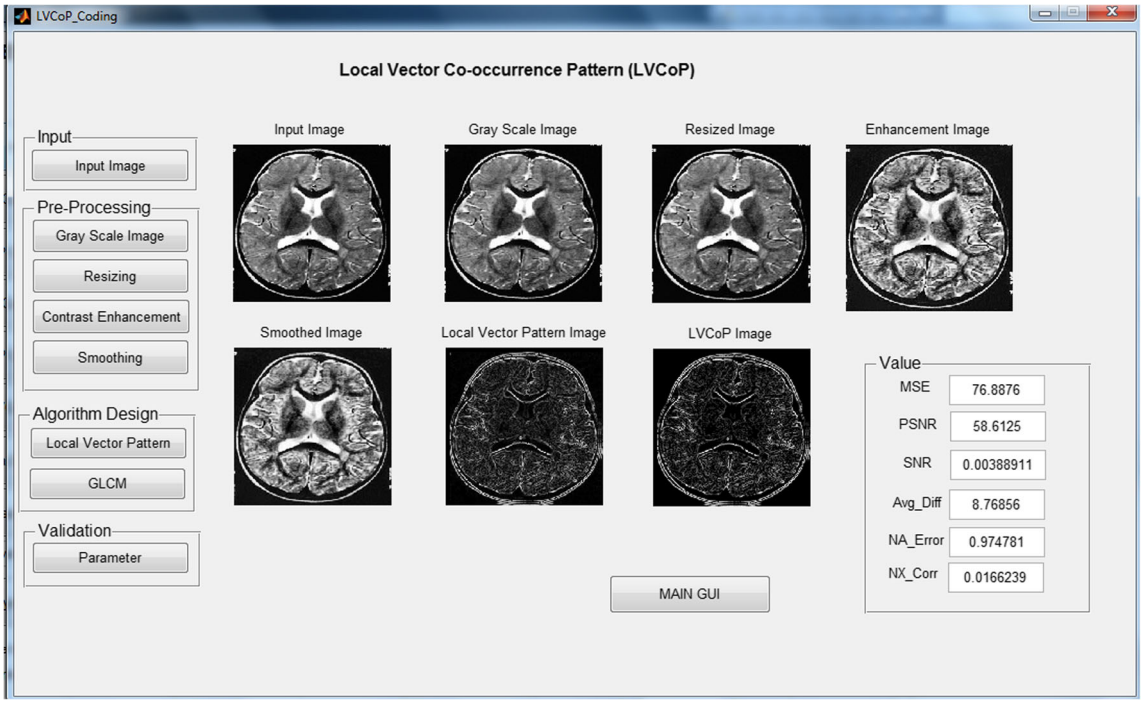

Fig. 2 The GUI for computing LVCoP

distance and sorted the values in ascending order. The image of the database which has very minimum difference or shorter distance attains a higher position and considered as the image having higher similarity. As per request from the user the retrieved images have been displayed in the main Graphical User Interface (GUI).

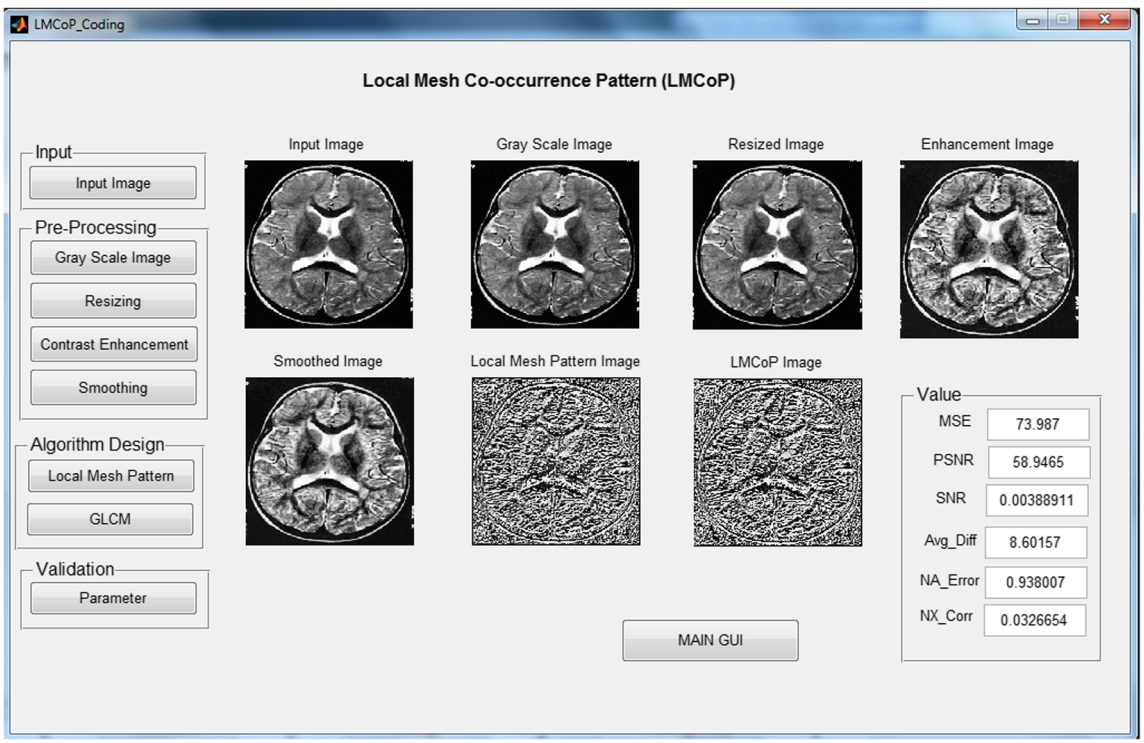

Fig. 3 The GUI for extracting features using LMCoP

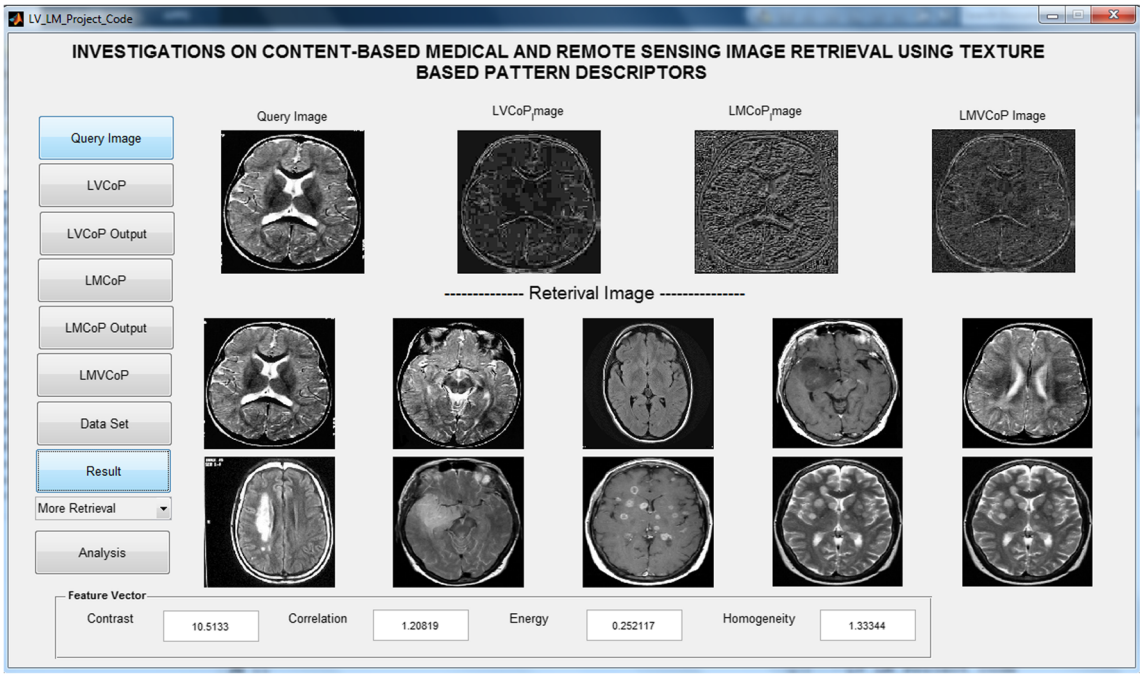

Fig. 4 The main GUI of proposed LMVCoP system showing the step-wise results and the first 10 retrieved MRI brain images

Step 6: Performance evaluation The effectiveness of the LMCoP and LVCoP techniques is evaluated using the following error sensitivity measures:

Mean Squared Error:

$$MSE(I,E) = \frac{1}{MN}\sum_{i=1}^{M}\sum_{j=1}^{N}\left(E_{i,j} - I_{i,j}\right)^2 \tag{17}$$

Peak Signal-to-Noise Ratio:

$$PSNR\ (I,E) = 10\ log\left(\frac{max\left(I^2\right)}{MSE(I,E)}\right) \tag{18}$$

Signal-to-Noise Ratio:

$$SNR(I,E) = 10\log\left(\frac{\sum_{i=1}^{M}\sum_{j=1}^{N}\left(I_{i,j}\right)^2}{M.N.MSE(I,E)}\right) \tag{19}$$

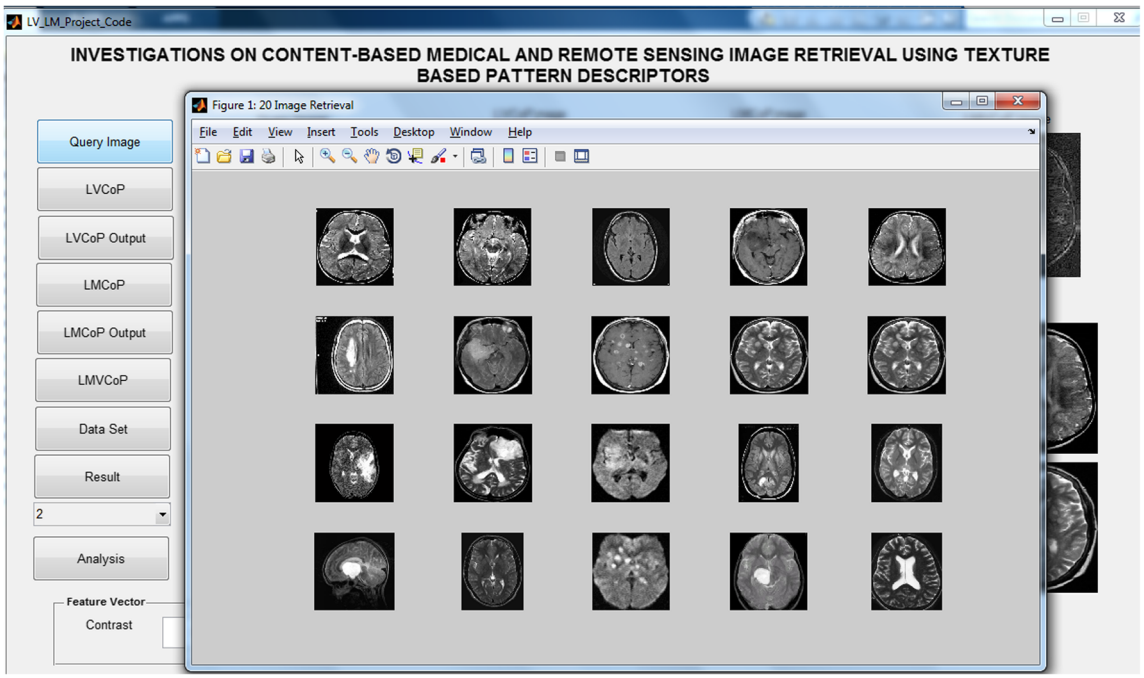

Fig. 5 A screen shot of retrieving top 20 images

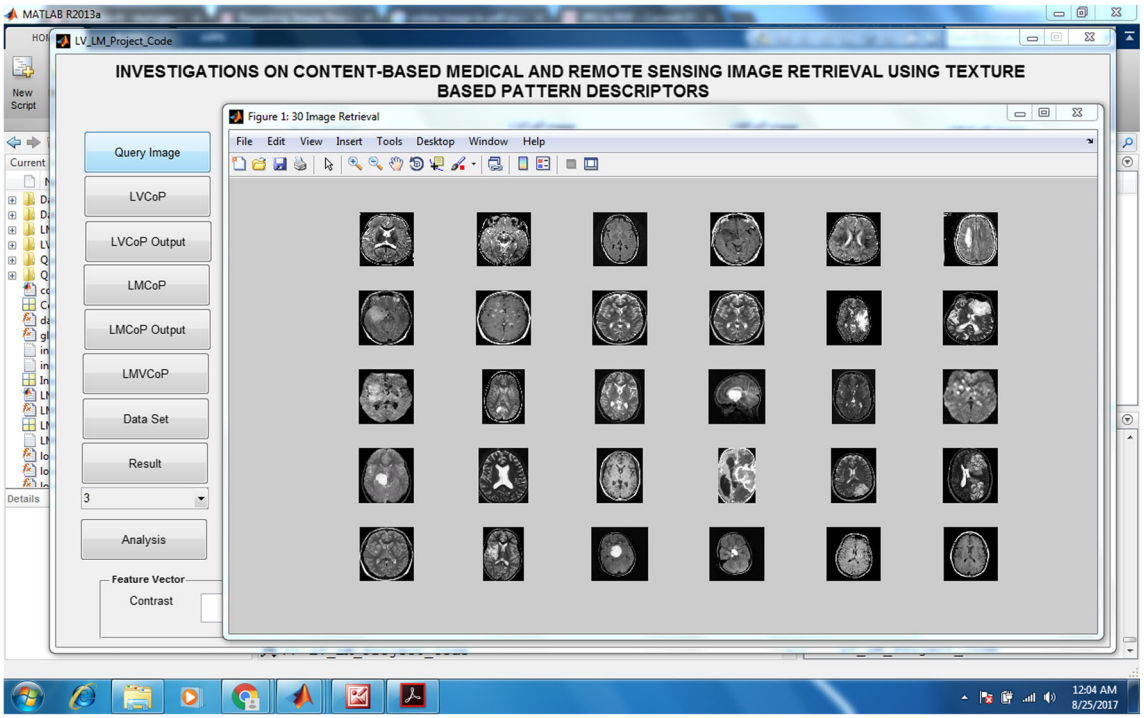

Fig. 6 A screen shot of retrieving top 30 images

Average Difference:

$$AD(I,E) = \frac{1}{MN}\sum_{i=1}^{M}\sum_{j=1}^{N}\left(I_{i,j} - E_{i,j}\right) \tag{20}$$

Normalized Absolute Error:

$$NAE(I,E) = \frac{\sum_{i=1}^{M}\sum_{j=1}^{N}\left|I_{i,j} - E_{i,j}\right|}{\sum_{i=1}^{M}\sum_{j=1}^{N}\left|I_{i,j}\right|} \tag{21}$$

Normalized Cross-Correlation:

$$NXC(I,E) = \frac{\sum_{i=1}^{M}\sum_{j=1}^{N}\left(I_{i,j}.E_{i,j}\right)}{\sum_{i=1}^{M}\sum_{j=1}^{N}\left(I_{i,j}\right)^2} \tag{22}$$

Table 1 Validation of LMCoP and LVCoP using Error Sensitivity measures

Quality Metric	LMCoP	LVCoP
MSE	0.967	0.8076
PSNR	54.5466	58.6125
SNR	0.00368911	0.00344711
AD	8.03974	8.23315
NAE	0.931171	0.976513
NXC	0.0313578	0.0116516

where, I is a given input image. E is the estimated or output image. $M \times N$ is the size of the image. The efficiency of the proposed image retrieval system is evaluated using the following performance evaluation metrics: Precision $P_j(M)$ is calculated by

$$P_j(M) = I_M/M \tag{23}$$

Whereas Recall, $R_j(M)$ is computed by

$$R_j(M) = I_M/S \tag{24}$$

Table 2 Haralick Features for the sample MRI brain Image based on LMVCoP

Image No.	LMVCoP			
	Contrast	Correlation	Energy	Homogeneity
1	10.5133	1.20819	0.252117	1.33344
2	16.7453	1.42222	0.144187	0.62786
3	20.4653	0.86786	0.787681	0.35555
4	14.5727	1.72678	0.418671	0.87878
5	21.2770	1.66645	0.874654	1.25786
6	12.0750	0.92154	0.835473	0.26788
7	19.5272	1.48795	0.157648	0.86289
8	18.2727	1.61475	0.218468	0.68876
9	25.7555	1.17498	0.174897	0.98698
10	17.7282	0.94184	0.614848	1.24554

Table 3 Time spent for Feature Extraction (FE) and Image Retrieval (IR) in seconds for OASIS-MRI database

Descriptors	FE	IR
LTCoP	22.20	0.61
PVEP	74.36	9.56
LMeP	12.60	1.42
LBDP	56.78	0.33
LVP	05.32	0.54
LMVCoP	04.29	0.21

Consider j^{th} dataset image is used as a query image. I_M is the number of relevant images retrieved, M is the total number of images retrieved and S is the total number of relevant images. The average precision $P_a^i(M)$ and average recall $R_a^i(M)$ for each class in the database are computed by

$$P_a^i(M) = \frac{1}{S}\sum_{j=1}^{S} P_j(M) \tag{25}$$

$$R_a^i(M) = \frac{1}{S}\sum_{j=1}^{S} R_j(M) \tag{26}$$

where i is the class number and a is the average. The Average Retrieval Precision (ARP) and Average Retrieval Rate (ARR) respectively were calculated using Eqs. (27 and 28).

$$P_a^T(M) = \frac{1}{C}\sum_{i=1}^{C} P_a^i(M) \tag{27}$$

Table 4 ARP based retrieval performance of all the methods on OASIS database (Group- wise)

Method	ARP (%) at $N = 10$				
	Group 1	Group 2	Group 3	Group 4	Total
LBP	54.91	34.80	33.96	51.79	44.72
GLBP	53.79	39.21	38.73	52.16	46.55
LTP	56.29	37.64	36.40	53.49	46.57
GLTP	51.53	35.09	33.38	45.09	41.60
LDP	46.29	36.37	36.82	45.56	41.80
GLDP	48.70	40.09	38.41	41.50	42.23
LTCoP	55.96	39.21	38.51	57.64	48.50
GLTCoP	65.16	45.09	44.07	71.41	57.22
LBPu2	51.77	32.54	33.82	49.06	42.63
LTPu2	53.38	38.23	36.61	53.39	45.81
GLTPu2	51.69	35.39	33.33	45.47	41.78
LDPu2	45.72	35.39	34.86	45.00	40.61
GLDPu2	45.8	39.80	37.19	43.49	41.37
LTCoPu2	55.88	40.29	36.56	57.35	47.57
GLTCoPu2	65.96	45.98	44.44	71.13	57.5
DBWPu2	52.74	37.74	34.38	60.00	47.05
LDMaMEP	66.77	45.98	41.73	76.99	57.87
LMeCH	70.32	45.49	42.35	77.73	60.26
LMVCoP	87.57	65.63	68.35	64.78	71.58

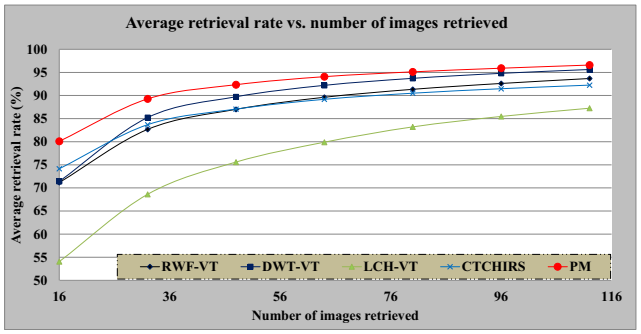

Fig. 7 The retrieval performances of the LMVCoP compared to LTCoP, PVEP, LMeP, LBDP and LVP methods in terms of ARP

$$R_a^T(M) = \frac{1}{C}\sum_{i=1}^{C} R_a^i(M) \tag{28}$$

where C is the total number of classes in the database. In this work, since the proposed LMVCoP is investigated only in MRI brain images, $C = 1$, Hence $P_a^i(M) = P_a^T(M)$ and $R_a^i(M) = R_a^T(M)$.

Results and discussion

The proposed LMVCoP is implemented in MATLAB software by building GUI in an Intel (R) Core i3 processor, 3.20 GHz, 4 GB RAM computer with the Microsoft Window7 Professional operation system platform. To test the efficiency of the proposed methodology a large data set of OASIS: MRI images [21] have been used in this work. There are four groups of dataset contain 106, 89, 102, and 124 MRI brain images were used for the test. For a data set, the evaluation is performed independently.

The proposed system interacts with the user through a succession of GUIs. First, in the pre-processing step, the given query image is converted into gray-scale image. After that, the scaling algorithm has been applied to resize the gray-scale image. Then, the image features have been enhanced with the help of contrast enhancement algorithm. Next, Gaussian smoothing is used to reduce the noise. Second, the features are extracted using the LVP and GLCM. Finally, LVCoP map is obtained. The results are shown as a snapshot in Fig. 2. The validation has been done

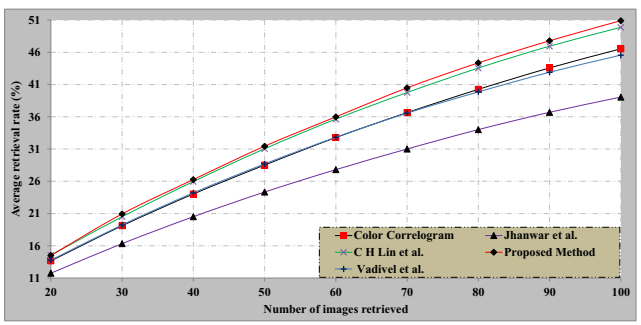

Fig. 8 The retrieval performances of the LMVCoP compared to LTCoP, PVEP, LMeP, LBDP and LVP methods in terms of ARR

using error sensitivity measures and values are displayed. After computing LVCoP, the function calls back to the main menu and the computation of LMCoP carries out as per the above-mentioned procedure. The results of LMCoP are shown in Fig. 3. The fusion of LVCoP and LMCoP are done and the LMVCoP features are generated and stored as feature vector database. The similarity between the features of database images and the query image are performed using Squared Euclidean distance and the retrieval images are displayed to the user. A screen shot of the results of top 10 retrieved images are shown in Fig. 4. Further, more number of (20 and 30) images are retrieved and displayed. A screen shot of the results of the various number of images retrieved are shown in Figs. 5 and 6 respectively.

The performance of LMCoP and LVCoP has been compared for a given input brain MRI image in terms of error sensitivity measures such as Mean Squared Error (MSE), Peak Signal-to-Noise Ratio (PSNR), Signal-to-Noise Ratio (SNR), Average Difference (AD), Normalized Absolute Error (NAE) and Normalized Cross Correlation (NXC) and the results are listed out in Table 1. When MSE is low, the PSNR value is high, then the quality rate turn into high. Here, PSNR is in the range of 50-60db. Hence, it is understood that the quality of processed image is high. Generally, SNR is defined as the power ratio and expressed in db. But, here it is expressed as the signal ratio. Hence, it is given in number. In general, there are 17 Haralick features. Out of 17 features, the Contrast, Correlation, Energy and Homogeneity features are considered as very important features that are obtained by Eqs, (7, 8, 11 and 12) and recorded in the Table 2. The contrast values reflect the sharp structural variations of medical images. The correlation imply that fine linear dependent features are present in the given images. The energy is used to measure texture crudeness; if it is equal for all the images, then it is concluded that the co-occurrence matrix has same values. But, from the values in Table 2, it is understood that the values of co-occurrence matrix are unequal. In view of the fact that the values of homogeneity of images #1, #5, #10 are nearer to 1 illustrate that they have diagonal GLCM. The Table 3 listed out the time spent for performing feature extraction and retrieval processes using the LMVCoP and the existing methods of LTCoP, PVEP, LMeP LBDP and LVP on bio-medical images. From Table 3, it is understood that the speed of feature extraction using LMVCoP is faster than the existing methods. Table 4 depicted the group-wise ARP based retrieval performance of all the state-of-the-arts of the LPD on the OASIS: MRI brain dataset. The comparison Table 4 depicts that the the LMVCoP outperforms in groups 1, 2 and 3. In group 4, GLTCoP, GLTCoPu2, LDMaMEP and LMeCH perform well than the proposed LMVCoP descriptor.

Figure 7 illustrates the performance of LMVCoP on OASIS: MRI brain images in terms of the ARP based on Squared Euclidean distance. It is evident that the average retrieval precision of LMVCoP, depicted in Fig. 7 is higher than all other existing methods. The high precision values obtained indicate that the LMVCoP is able to retrieve more relevant images. The ARR result exposed in Fig. 8 illustrates that as precision increases, the recall value decreases. Hence, it is known that the LMVCoP has given better performance. The proposed LMVCoP descriptor achieved the ARP of 87.57% and the ARR of 53.21% for the first 10 number of retrieval images.

Conclusions

In this paper, the LMVCoP descriptor has been proposed to obtain better retrieval performance on medical images for the fast decision making in clinical application. The LMVCoP extracted the texture features of the MRI brain images by concatenating the LPD and GLCM. The performance of LMVCoP has been compared in terms of performance evaluation metrics with the existing descriptors that were used for biomedical indexing and retrieval such as LTCoP, PVEP, LMeP, LBDP and LVP. LMVCoP descriptor achieves 87.57% of ARP and 53.21% of ARR. The time spent by LMVCoP descriptors for feature extraction is 04.29 s and retrieval is 0.21 s that were also less. The simulation results and investigations prove that the LMVCoP outperforms the LTCoP by 31.61%, the PVEP by 17.43%, the LMeP by 6.21%, the LBDP by 4.6%, and the LVP by 4.05% in terms of ARP. Implementing higher-order LMVCoP is an immediate challenge. In future, it is planned to implement higher order LMVCoP and to combine LPDs and neural network methods for retrieving large-scale high dimentional image datasets.

Compliance with ethical standards

Conflict of interest The authors declare that they have no conflict of interest.

Human and animal rights and informed consent This article does not contain any studies with human participants or animals performed by any of the authors.

References

1. Duncan, J.S., and Ayache, N., Medical image analysis: Progress over two decades and the challenges ahead. *IEEE Trans. Pattern Anal. Mach. Intell.* 22(1):85–106, 2000.
2. Iakovidis, D., Pelekis, N., Kotsifakos, E., Kopanakis, I., Karanikas, H., and Theodoridis, Y., A pattern similarity scheme for medical image retrieval. *IEEE Trans. Inf. Technol. Biomed.* 13(4):442–450, 2009.
3. Rahman, M. M., Antani, S. K., Long, R. L., Demner, D-F., and Thoma, G. R., Multi-Modal Query Expansion Based on Local Analysis for Medical Image Retrieval. *Medical Content-Based Retrieval for Clinical Decision Support*. Berlin, Springer; 110–119, 2010.
4. Wang, J., Li, Y., Zhang, Y., Wang, C., Xie, H., Chen, G., and Gao, X., Bag-of-features based medical image retrieval via multiple assignment and visual words weighting. *IEEE Trans. Med. Imag.* 30(11):1996–2011, 2011.

5. Quellec, G., Lamard, M., Cazuguel, G., Roux, C., and Cochener, B., Case retrieval in medical databases by fusing heterogeneous information. *IEEE Trans. Med. Imag.* 30(1):108–118, 2011.
6. Cao, Y., Steffey, S., He, J., Xiao, D., Tao, C., Chen, P., and Müller, H., Medical Image Retrieval: A Multimodal Approach. *Cancer Informat.* 13(S3):125–136, 2014.
7. Zehra, C., Amlica, H., Tizhoosh, R., and Khalvati, F., Medical Image Classification via SVM using LBP Features from Saliency-Based Folded Data, *Proceedings of the 14th International Conference on Machine Learning and Applications (IEEE ICMLA'15)*, Miami, Florida, USA, (pp 1–5), 2015.
8. Albarqouni, S., Baur, C., Achilles, F., Belagiannis, V., Demirci, S., and Navab, N., AggNet: Deep learning from crowds for mitosis detection in breast cancer histology images. *IEEE Trans. Med. Imag. Special Issue on Deep Learning*. 35(5):1313–1321, 2016.
9. Ngan, T.T., Tuan, T.M., Son, L.H., Minh, N.H., and Dey, N., Decision making based on fuzzy aggregation operators for medical diagnosis from dental X-ray images. *J Med Syst.* 40:280, 2016.
10. Govindaraju, S., and Ramesh Kumar, G.P., A novel content based medical image retrieval using SURF features. *Indian J. Sci. Technol.* 9(20):1–8, 2016.
11. Liu, X., Tizhoosh, H. R., and Kofman, J., Generating Binary Tags for Fast Medical Image Retrieval Based on Convolutional Nets and Radon Transform. *Proceedings of the 2016 I.E. International Joint Conference on Neural Networks (IJCNN 2016)*, Vancouver, Canada, (pp. 1–7), 2016.
12. Meena, P.R., and Shantha, S.R., Spatial fuzzy C means and expectation maximization algorithms with bias correction for segmentation of MR brain images. *J. Med. Syst.* 41:15, 2017.
13. Ojala, T., Pietikäinen, M., and Harwood, D., A comparative study of texture measures with classification based on featured distribution. *Pattern Recognit.* 29(1):51–59, 1996.
14. Tan, X., and Triggs, B., Enhanced local texture feature sets for face recognition under difficult lighting conditions. *IEEE Trans. Image Process.* 19(6):1635–1650, 2010.
15. Murala, S., Maheshwari, R.P., and Balasubramanian, R., Local tetra patterns: A new descriptor for content-based image retrieval. *IEEE Trans Image Process.* 21(5):2874–2886, 2012.
16. Murala, S., Maheshwari, R.P., and Balasubramanian, R., Directional binary wavelet patterns for biomedical image indexing and retrieval. *J. Med. Syst.* 36(5):2865–2879, 2012.
17. Murala, S., and Wu, Q. M. J., Peak Valley Edge Patterns: A New Descriptor for Biomedical Image Indexing and Retrieval. *Proc. IEEE CVPR Workshops* (pp. 444-449), 2013.
18. Murala, S., and Wu, Q.M.J., Local mesh patterns versus local binary patterns: Biomedical image indexing and retrieval. *IEEE J. Biomed. Health Inform.* 18(3):929–938, 2014.
19. Fan, K.-C., and Hung, T.-Y., A novel local pattern descriptor-local vector pattern in high-order derivative space for face recognition. *IEEE Trans. on Image Process.* 23(7):2877–2891, 2014.
20. Yesubai, R. C., and Ravi, R., Local mesh co-occurrence pattern for content based image retrieval. Inte. J. Comput. Electr. Autom. Control Info. Eng. 9(6): 1510–1515, 2015.
21. Marcus, D.S., Wang, T.H., Parker, J., Csernansky, J.G., Morris, J.C., and Buckner, R.L., Open access series of imaging studies (OASIS): Cross-sectional MRI data in young, middle aged, nondemented, and demented older adults. *J. Cogn. Neurosci.* 19(9): 1498–1507, 2007.